Available online at www.sciencedirect.com
ScienceDirect
Journal of Solid State Chemistry 180 (2007) 1340–1346
JOURNAL OF SOLID STATE CHEMISTRY
www.elsevier.com/locate/jssc

Hydrothermal synthesis and magnetic properties of $R\mathrm{Mn_2O_5}$ (R = La, Pr, Nd, Tb, Bi) and $\mathrm{LaMn_2O_{5+\delta}}$

Yan Chen, Hongming Yuan, Ge Tian, Ganghua Zhang, Shouhua Feng*

State Key Laboratory of Inorganic Synthesis and Preparative Chemistry, College of Chemistry, Jilin University, Changchun 130023, PR China

Received 1 November 2006; received in revised form 5 February 2007; accepted 8 February 2007
Available online 20 February 2007

Abstract

$R\mathrm{Mn_2O_5}$ (R = La, Pr, Nd, Tb, Bi) crystallites were prepared by a mild hydrothermal method and characterized by powder X-ray diffraction, scanning electron microscopy, X-ray photoelectron spectroscopy (XPS) and magnetic measurement. The formation of manganates was sensitive to the alkalinities and Mn-containing precursors of the reaction mixtures. This family of manganates is isostructural and has a space group of *Pbam*. The magnetic measurements for $R\mathrm{Mn_2O_5}$ showed an antiferromagnetic transition. The strong irreversibility between the ZFC and FC curves indicated a helicoidally magnetic structure below 40 K. The max d.c. susceptibilities of $\mathrm{LaMn_2O_{5+\delta}}$ ($\delta = 0.01, 0.06, 0.08, 0.16, 0.17$) were found to be variable and the excess oxygen (δ) in the compounds was influenced by the alkalinity used in the hydrothermal synthesis.

Keywords: Hydrothermal synthesis; $R\mathrm{Mn_2O_5}$; Birnessite gel

1. Introduction

The discovery of colossal magnetoresistance effect in the hole-doped rare-earth manganites $R_{1-x}A_x\mathrm{MnO_3}$ (R denotes rare-earth ions and A denotes alkaline earth ions) has originated a great interest in the study of the mixed-valence transition metal oxides [1]. $R\mathrm{Mn_2O_5}$ represents a family of compounds that contains Mn^{3+} and Mn^{4+} ions in two crystallographic sites. Pure phases were firstly prepared from $\mathrm{Bi_2O_3}$ flux [2,3]. The crystal structure of $R\mathrm{Mn_2O_5}$ is orthorhombic (space group *Pbam*) and consists of the octahedrally coordinated Mn^{4+} (4*f*) and square-planar pyramid Mn^{3+} (4*h*) [4]. Neutron diffraction studies showed that the magnetic structure is rather complex and magnetic moments of Mn^{3+} and Mn^{4+} ions form a helical magnetic ordering below T_N [5,6].

Normally, the mixed-valence manganese oxides are prepared by traditional high-temperature solid-state reaction. However, high oxygen pressure is still necessary in the synthesis of single-phased $R\mathrm{Mn_2O_5}$. Some alternative synthetic routes, such as fused-salt electrolysis, SHS and citrate-gel methods, have been studied to prepare such manganese oxides at relatively lower temperature. The mild hydrothermal method is an attractive route to prepare the inorganic solids due to the relatively mild conditions, one-step synthetic procedure and controllable particle size distribution [7–9]. This method has been widely used in the preparation of manganese oxide molecular sieves (OMS) and $A_x\mathrm{MnO_2}$ oxides, which have open crystalline structures or expandable layered structures [10–13]. Recently, a series of the hole-doped manganates $R_{0.5}A_{0.5}\mathrm{MnO_3}$ (R = La, Pr, Nd; A = Ca, Ba, Sr) were hydrothermally synthesized with high alkalinity [14–18]. We have successfully synthesized polycrystalline manganates by hydrothermal treatment of the mixture of rare-earth oxides, K-birnessite gel and KOH. As an extension of our study, we report here the hydrothermal synthesis and magnetic properties of $R\mathrm{Mn_2O_5}$ (R = La, Pr, Nd, Tb and Bi).

2. Experimental

In a typical synthetic procedure for $Ln\mathrm{Mn_2O_5}$ (Ln = La, Pr, Nd, Tb or Bi), 10 g KOH was dissolved in 40 mL 0.06 M $\mathrm{KMnO_4}$ solution with stirring, into which 26 mL

*Corresponding author. Fax: +86 431 516 8624.
E-mail address: shfeng@mail.jlu.edu.cn (S. Feng).

0022-4596/$ - see front matter © 2007 Elsevier Inc. All rights reserved.
doi:10.1016/j.jssc.2007.02.005

0.28 M $MnCl_2$ was added dropwise in an ice bath. Finally, 50 g KOH and 0.8 g R_2O_3 (R = La, Nd, Bi; Tb_4O_7; Pr_6O_{11}) were added to form the reaction mixtures (KOH concentration was 13.4 M).

After stirring with a magnetic stirrer for 30 min, the reaction mixtures were transferred to Teflon-lined stainless steel autoclaves with a filling capacity of 80%. The crystallization was carried out under autogenous pressure at 240 °C for 3 days. Dark powder products were filtered and washed with distilled water and sonicated by a direct immersion titanium horn (Vibracell, 20 kHz, 200 W/cm^2).

X-ray diffraction (XRD) data were collected using a Rigaku D/Max 2550 V/PC X-ray diffractometer with CuKα radiation ($\lambda = 1.5418$ Å) of 40 kV and 250 mA at room temperature by step scanning in the angle range $10^\circ \leqslant 2\theta \leqslant 120^\circ$ with increments of 0.02°. Scanning electron microscopy (SEM) was performed with a Rigaku JSM-6700F microscope operated at 10 kV. The magnetic properties of the compounds were studied by measuring the sample magnetization as a function of applied magnetic field by SQUID (Quantum Design, MPMS-LX). X-ray photoelectron spectroscopy (XPS) was performed using AlKα radiation from a VG ESCALAB MK-II X-ray photoelectron spectrometer. The d.c. susceptibility measurements, both under zero-field-cooling (ZFC) and field-cooling (FC) conditions, were performed in a 0.1 kOe magnetic field for temperatures ranging from 4 to 300 K. An isothermal magnetization curve was obtained in a magnetic field up to 50 kOe.

3. Results and discussion

The room-temperature powder XRD patterns of RMn_2O_5 (R = La, Pr, Nd, Tb, Bi) are shown in Fig. 1. The XRD patterns were well indexed in an orthorhombic unit cell of space group *Pbam*, with no additional peaks which could indicate the presence of superstructures or departure from the mentioned symmetry. The indexed XRD reflections of $LaMn_2O_5$ were taken as an example as shown in Fig. 2. Lattice parameters of RMn_2O_5, listed in Table 1, were refined by the Rietveld method taking as starting structural model that of $NdMn_2O_5$ [19]. SEM pictures in Fig. 3 show that all the products are crystalline and some of them show nanocrystalline characteristics, such as in the case of $TbMn_2O_5$ (see Fig. 3F). Furthermore, $LaMn_2O_{5+\delta}$ ($\delta = 0.01$, 0.06, 0.08, 0.16, 0.17) can be hydrothermal synthesized with different alkalinity. XRD, XPS and SEM for $LaMn_2O_{5+\delta}$ are given in Supporting information.

In the past few years, many transition metal oxides, such as $LaCrO_3$, $BiFeO_3$ and doped manganates $R_{0.5}A_{0.5}MnO_3$, were successfully synthesized by mild hydrothermal treatment of the mixtures of metal salts in potassium hydroxide solution [8,14–18,27–29,33]. Recently, lots of nano-scale oxides have been prepared by the method [30–32]. The most typical example is the TiO_2 nanotube prepared by hydrothermal treatment of amorphous TiO_2 with a solution of NaOH (10 mol/dm^3) [35]. The common character of the mild hydrothermal synthesis of such oxides is the high alkalinity of the solution. KOH or NaOH

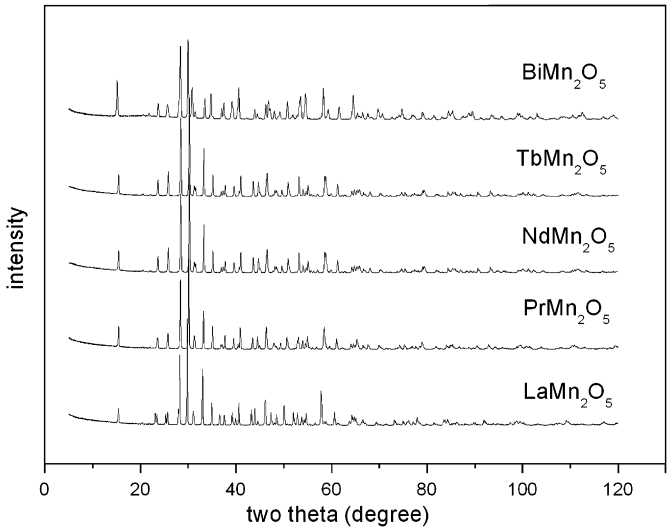

Fig. 1. XRD patterns of RMn_2O_5 (R = La, Pr, Nd, Tb, Bi).

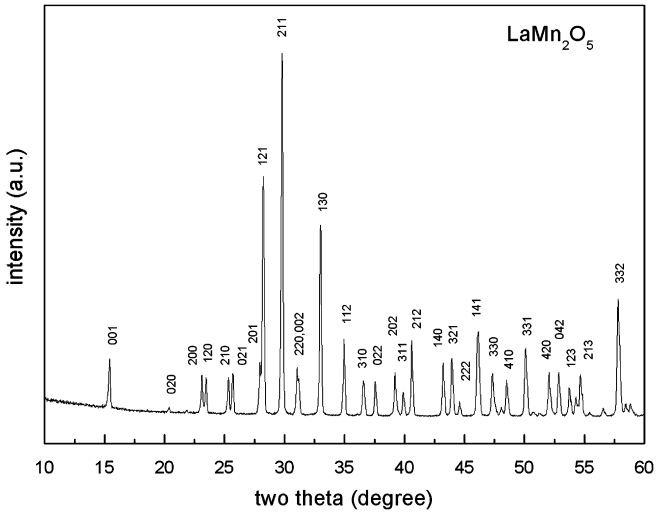

Fig. 2. Indexing of the XRD pattern of $LaMn_2O_5$, according to an orthorhombic unit cell with dimensions $a = 7.6724(4)$ Å, $b = 8.6829(3)$ Å and $c = 5.722(2)$ Å.

Table 1
Unit cell parameters and volume for the manganates RMn_2O_5 determined from Rietveld refinement of XRD data at room temperature

Composition	a (Å)	b (Å)	c (Å)	V (Å^3)
$LaMn_2O_5$	7.677(2)	8.690(2)	5.725(1)	381.93
$PrMn_2O_5$	7.562(1)	8.657(1)	5.7172(9)	372.27
$NdMn_2O_5$	7.501(1)	8.620(2)	5.701(1)	368.61
$TbMn_2O_5$	7.3222(5)	8.5221(6)	5.6768(4)	354.23
$BiMn_2O_5$	7.556(2)	8.533(2)	5.761(2)	371.44

Details of refined parameters of Rietveld refinement are listed in supporting information.

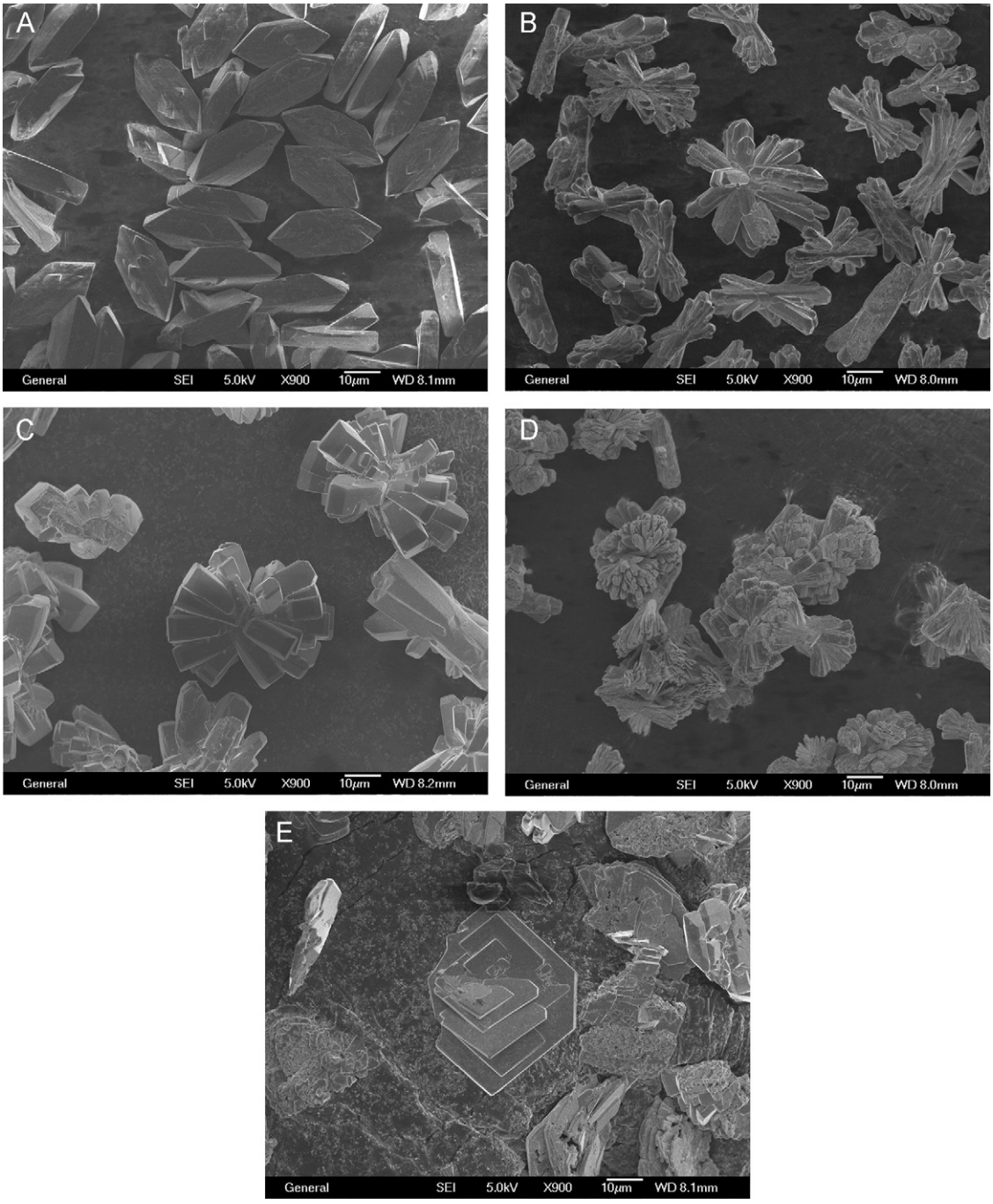

Fig. 3. SEM pictures of RMn_2O_5 (R = La, Pr, Nd, Tb, Bi) for (A) $LaMn_2O_5$, (B) $PrMn_2O_5$, (C) $NdMn_2O_5$, (D) $TbMn_2O_5$, (E) $BiMn_2O_5$ and (F) one-dimensional nanostructure of $TbMn_2O_5$.

was used to maintain the alkalinity (KOH or NaOH concentration usually above 7 M). Such high alkalinity provides a critical condition which considerably influences the crystallization and composition of the product in hydrothermal synthesis. For example, we have successfully synthesized a series of $Pr_{1-x}Ca_xMnO_3$ with variable doping rate in the previous work. It was founded that the different KOH concentration dominates the crystallization and formation of $Pr_{1-x}Ca_xMnO_3$ with a purposed doping rate [36].

In our experiments, we assume that $R(OH)_3$ is formed from R_2O_3 in hydrothermal condition at first, then it dissolves in strong alkaline-aqueous medium and reacts with K-birnessite gel. To confirm this assumption, $R(NO_3)_3$ instead of R_2O_3 were mixed with K-birnessite gel in strong alkaline solution. $R(OH)_3$ was formed immediately when $R(NO_3)_3$ was added into the alkaline solution. The RMn_2O_5 compounds can be reproduced by hydrothermal treatment of the mixture as well. Although the solubility of $R(OH)_3$ in the alkaline solution decreases with the increase

of reaction temperature, the high reaction temperature (above 240 °C) can promote the reaction of K-birnessite gel with $R(OH)_3$ and crystallization of the product in hydrothermal synthesis. The product can be synthesized over a wide range of KOH concentration (8–14 M) with a little $K_xMnO_2 \cdot 0.5$–$0.7H_2O$ as impurity. After sonication, single-phase RMn_2O_5 was obtained as fine dark polycrystalline powder at the bottom of the beaker.

The Mn-containing precursor is one of the critical factors which dominate the formation of RMn_2O_5 in the

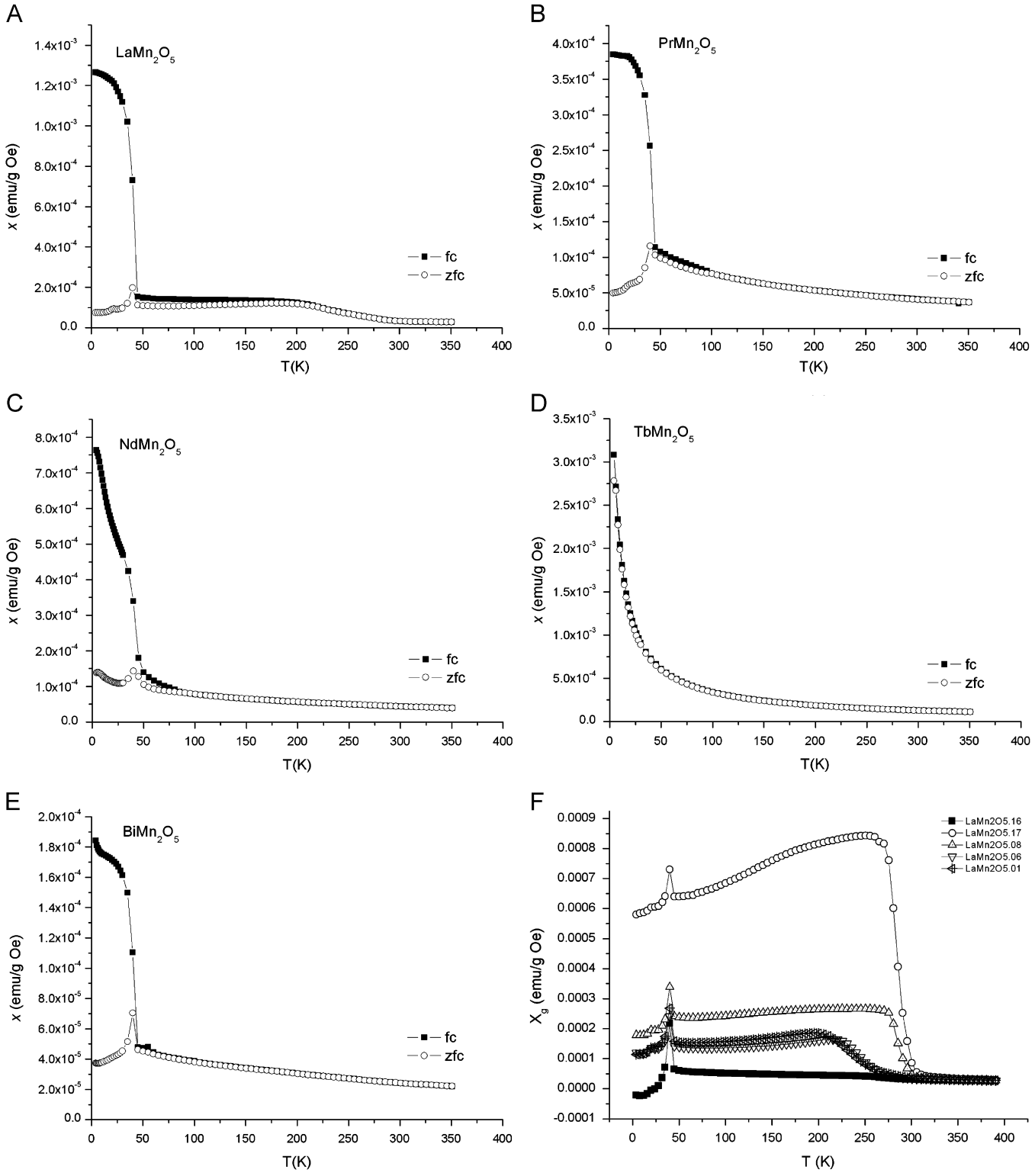

Fig. 4. The d.c. magnetic curves of RMn_2O_5 (R = La, Pr, Nd, Tb, Bi) hydrothermally synthesized with 13.4 M KOH solution for (A) $LaMn_2O_5$, (B) $PrMn_2O_5$, (C) $NdMn_2O_5$, (D) $TbMn_2O_5$, (E) $BiMn_2O_5$ and (F) ZFC curve of $LaMn_2O_{5+\delta}$ synthesized under different KOH concentration.

synthesis. Usually, hydrothermal transformation of layered manganese oxide materials (birnessite, etc.) is one of the most effective methods of obtaining tunnel-structured manganese oxides and OMS [20–22]. Birnessite has an octahedral layer (OL-1) structure, in which metal ions and water molecules locate. In our recent research, birnessite-like precursor (K-birnessite mixed with a little Mn_3O_4 as impurity) formed when $KMnO_4$ solution mixed with $MnCl_2$ solution in the synthesis of the variable doping-rate manganite perovskites $Pr_{1-x}Ca_xMnO_3$ ($x = 0.2$, 0.3, 0.5, 0.6) [36]. Hydrothermal transformation of birnessite precursor plays an important role in the preparation of mixed-valence manganese oxides, because the framework manganese of birnessite, usually (+2, +3, +4) or (+3 and +4), can easily transform to mixed-valent manganese in the products. The K-birnessite gel, synthesized by the redox reaction of $KMnO_4$ with $MnCl_2$ in an ice bath [11,12], was used in the hydrothermal synthesis of RMn_2O_5 manganates as the Mn source.

The bulk magnetic susceptibility is used for characterizing the feature of magnetic ordering of a material. The d.c. magnetic susceptibilities of the different members in the RMn_2O_5 family are shown in Fig. 4. The magnetic properties of the RMn_2O_5 (R = La, Pr, Nd, Bi) samples reveal that these oxides have similar antiferromagnetic properties at low temperatures and Neel temperature (T_N) depends on the nature of rare-earth ions. The result of previous investigation of powder neutron diffraction showed that Mn^{3+} and Mn^{4+} ordering moments are helicoidally arranged in the *ab* plane for RMn_2O_5 family [4,34]. The helical order can occur in a crystal when exchange interactions act not only between ions within the same layer and between those in nearest-neighboring layers, but also between ions in next-nearest layers, and beyond [32]. Inhomogeneous magnetic behavior is observed in the RMn_2O_5 (R = La, Pr, Nd, Bi), since the susceptibility curves present clear diversity between ZFC and FC curves below 40 K, which is caused by the helicoidally magnetic structure of the compounds [25]. In

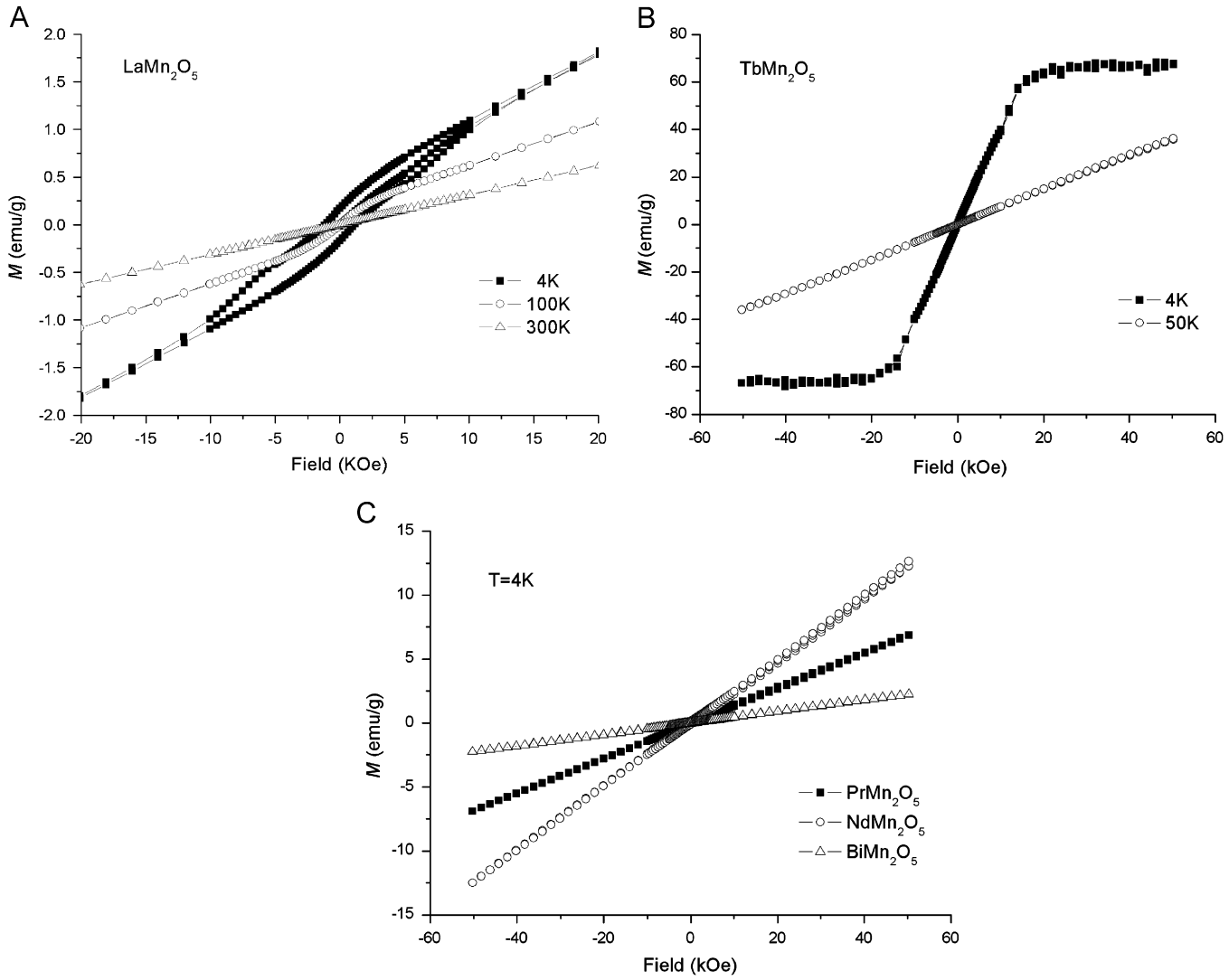

Fig. 5. Isothermal magnetic curves of RMn_2O_5 (R = La, Pr, Nd, Tb, Bi) for (A) $LaMn_2O_5$, (B) $TbMn_2O_5$, (C) $PrMn_2O_5$, $NdMn_2O_5$ and $BiMn_2O_5$.

Fig. 5, the magnetization isothermal for $LaMn_2O_5$ suggests weak ferromagnetic property, which is canted-antiferromagnetic coupling. The spin-glass-like phase would not be expected in our sample of $LaMn_2O_5$, since its imaginary part of a.c. susceptibility has no response, which is different from the reported spin glass behavior of $LaMn_2O_5$ synthesized by citrate technique [4].

We noticed that $TbMn_2O_5$ presents quite different magnetic behavior from other RMn_2O_5 (R = La, Pr, Nd, Bi), which is originated from the magnetic property of the heavy rare-earth Tb cation at low temperature. It is well known that Tb^{3+} ion has the $(4f)^8$ electronical configuration and a magnetic moment of $9.7\,\mu_B$ with a large magnetic anisotropy. The negative Curie–Weiss constant ($\theta = -15$) indicates the typical antiferromagnetic property of the compound. No inhomogeneous magnetic behavior was observed in d.c. measurement of $TbMn_2O_5$ [23,24]. The isothermal magnetization for $TbMn_2O_5$, presented in Fig. 4b, exhibits a tendency to saturation at higher magnetic fields, which is due to the strong anisotropy of Tb^{3+} at low temperature [26].

Table 2 summarizes the magnetic parameters of RMn_2O_5 (R = La, Pr, Nd, Bi, Tb). The effective paramagnetic moment of RMn_2O_5 determined at high temperatures is in excellent agreement with that calculated with the formula: $\mu_{cata} = (\mu(R^{3+})^2 + \mu(Mn^{3+})^2 + \mu(Mn^{4+})^2)^{1/2}$. For Mn^{3+} ion ($3d^4$, high-spin state, $S = 2$, $g_J = 2$), the theoretical spin-only value is $\mu_{eff} = g_J[S(S+1)]^{1/2}\,\mu_B = 4.90\,\mu_B$. For Mn^{4+} ions ($3d^3$, low-spin state, $S = 1.5$, $g_J = 2$), the value is $\mu_{eff} = 3.87\,\mu_B$. Our experimental data is in good agreement with the calculated value, which confirms that the ratio of Mn^{3+} and Mn^{4+} in the compounds is close to 1:1. Deviations from the expected values may be explained by excess oxygen in the compounds. Alonso et al. have suggested that the best formulation of this compound is $RMn_2O_{5+\delta}$, whose δ indicates the excess oxygen in the structure [23]. We have reported that the thermal and XPS analysis of $LaMn_2O_{5+\delta}$ show that the oxidation state of manganese is slightly higher than the expected value 3.5 and is variable with concentration of KOH in hydrothermal synthesis [18].

To study the relationship between the magnetic property and the oxygen excess, a series of $LaMn_2O_{5+\delta}$ were obtained by using different concentration of alkalinity in the synthesis. Their value of oxygen excess (δ) was determined by Gaussian fitting XPS spectrum [18]. It is worthwhile to note that the value of excess oxygen decreases when the concentration of alkalinity increases above 7.8 M as listed in Table 3. The d.c. magnetic measurement of the samples shows the existence of transition from paramagnetic to antiferromagnetic as shown in Fig. 4F. The max susceptibility of the ZFC curve is observed in the $LaMn_2O_{5.17}$ which was prepared with 8.9 M KOH concentration in hydrothermal synthesis. The sharp increase around 300 K in the ZFC curve implies canted-antiferromagnetic coupling which is due to the strong sublattice cant in $LaMn_2O_{5.17}$. Such behavior suggests that the magnetic properties of $LaMn_2O_{5+\delta}$ are sensitive to the excess oxygen (δ).

Table 2
Magnetic constants for RMn_2O_5 hydrothermal synthesized with 13.4 M KOH, calculated from magnetic susceptibility data

Compound	μ_{cata}[a] (high-spin state for Mn^{3+})	μ_{obs}	C (emu K/g)	θ_p (K)	T_N (K)
$LaMn_2O_5$	6.24	6.28	0.015	−192	200
$PrMn_2O_5$	7.20	6.70	0.017	−132	100
$NdMn_2O_5$	7.22	7.31	0.020	−154	75
$TbMn_2O_5$	11.55	10.70	0.041	−15	–
$BiMn_2O_5$	6.24	6.43	0.013	−233	60

The paramagnetic moments per formula unit are given in μ_B.
[a]$\mu_{cata} = (\mu(R^{3+})^2 + \mu(Mn^{3+})^2 + \mu(Mn^{4+})^2)^{1/2}$.

Table 3
Mean valence of hydrothermally synthesized $LaMn_2O_{5+\delta}$

Compound Mn	KOH concentration (M)	Mean valence of XPS[a]
$LaMn_2O_{5.16}$	7.8	3.66
$LaMn_2O_{5.17}$	8.9	3.67
$LaMn_2O_{5.08}$	10	3.58
$LaMn_2O_{5.06}$	11	3.56
$LaMn_2O_{5.01}$	13.4	3.51

[a]Detail information is given in supporting information.

4. Conclusions

A series of polycrystalline RMn_2O_5 (R = La, Pr, Nd, Bi, Tb) were synthesized through hydrothermal treatment of K-birnessite gel precursor mixed with rare-earth oxides in high alkaline solution. This method is advantageous due to the mild conditions required, one-step synthetic procedure and easy handling. The high alkalinity of the reaction system supplies a critical condition considerably influencing the crystallization and composition of the products. Among these RMn_2O_5 samples, crystal of $LaMn_2O_5$ was formed in good shape and $TbMn_2O_5$ was comprised of one-dimensional nanostructure. Magnetic properties of RMn_2O_5 depended on the nature of the rare-earth elements.

Acknowledgments

This work was supported by the National Natural Science Foundation of China (nos. 20121103 and 20631010) and 863 program.

Appendix A. Supporting information

Supplementary data associated with this article can be found in the online version at doi:10.1016/j.jssc.2007.02.005.

References

[1] R.V. Helmholt, J. Wecker, B. Holzapfel, L. Schultz, K. Samwer, Phys. Rev. Lett. 71 (1993) 2331.
[2] S. Quezel-Ambrunaz, E.F. Bertaut, G. Buisson, CR Acad. Sci. Paris 258 (1964) 3025.
[3] E.F. Bertaut, G. Buisson, A. Durif, A. Mareschat, M.C. Montmory, S. Quezel-ambrunaz, Bull. Soc. Chim. Fr. (1965) 1132.
[4] J.A. Alonso, M.T. Casais, M.J. Martínez-Lope, J.L. Martínez, M.T. Fernández-Díaz, J. Phys.: Condens. Matter 9 (1997) 8515.
[5] C. Wilkinson, F. Sinclair, P. Gardner, J.B. Forsyth, B. Wanklyn, J. Phys. C Solid State Phys. 14 (1981) 1671.
[6] I. Kagomiya, H. Kimura, Y. Noda, K. Kohn, J. Phys. Soc. Jpn. 70 (Suppl. A 145) (2001).
[7] D. Wang, R. Yu, S. Feng, W. Zheng, R. Xu, N. Kumada, N. Kinomura, Mater. Res. Bull. 36 (2001) 239.
[8] D. Wang, R. Yu, N. Kumada, N. Kinomura, Chem. Mater. 12 (2000) 956.
[9] S.H. Feng, R.R. Xu, Acc. Chem. Res. 34 (2001) 239.
[10] R. Chen, P. Zavalij, M.S. Whittingham, Chem. Mater. 6 (1996) 1275.
[11] X.F. Shen, Y.S. Ding, J. Liu, J. Cai, K. Laubernds, R.P. Zerger, A. Vasiliev, M. Aindow, S.L. Suib, Adv. Mater. 17 (2005) 805.
[12] J. Morales, L. Sa′nchez, S. Bach, J.P. Pereira-Ramos, Mater. Lett. 56 (2002) 653.
[13] Y.H. Xu, Q. Feng, K. Kajiyoshi, K. Yanagisawa, Chem. Mater. 14 (2002) 697.
[14] J. Spooren, A. Rumplecker, F. Millange, R.I. Walton, Chem. Mater. 15 (2003) 1401.
[15] J. Spooren, R.I. walton, F. Millange, J. Mater. Chem. 15 (2005) 1542.
[16] J. Spooren, R.I. Walton, J. Solid State Chem. 178 (2005) 1683.
[17] Y.W. Wang, X.Y. Lu, Y. Chen, F.L. Chi, S.H. Feng, J. Solid State Chem. 178 (2005) 1317.
[18] H. Zhao, S. Gao, Y. Li, S.L. Liu, S.H. Feng, J. Mater. Chem. 13 (2003) 852.
[19] H.M. Rieveld, J. Appl. Crystallogr. 2 (1969) 65.
[20] S.L. Brock, M. Sanabria, J. Nair, S.L. Suib, T. Ressler, J. Phys. Chem. B 105 (2001) 5404.
[21] Y.F. Shen, R.P. Zerger, S.L. Suib, McCurdy, L. Potter, D.I. O'Young, Chem. Commun. 17 (1992) 1213.
[22] Y.F. Shen, R.P. Zerger, R.N. DeGuzman, S.L. Suib, McCurdy, L. Potter, D.I. O'Young, Science 260 (1993) 511.
[23] J.A. Alonso, M.T. Casais, M.J. Martinez-Lope, I. Rasines, J. Solid State Chem. 129 (1997) 105.
[24] I. Kagomiya, K. Kohn, T. Uchiyama, Ferroelectrics 280 (2002) 131.
[25] A. Inomata, K. Kohn, J. Phys. Condens. Matter 8 (1996) 2673.
[26] K. Saito, K. Kohn, J. Phys. Condens. Matter 7 (1995) 2855.
[27] W.J. Zheng, W.Q. Pang, G.Y. Meng, D.K. Peng, J. Mater. Chem. 9 (1999) 2833.
[28] M. Wu, J. Long, G. Wang, A. Huang, Y. Luo, S.H. Feng, R.R. Xu, J. Am. Ceram. Soc. 82 (1999) 3254.
[29] Y.H. Shi, S.H. Feng, J.X. Li, C.R. zhang, W.F. Li, Chem. J. Chinese Univ. 20 (1999) 172.
[30] J.B. Liu, H. Wang, M.K. Zhu, B. Wang, H. Yan, Mater. Res. Bull. 38 (2002) 817.
[31] T. Zhang, C.G. Jin, T. Qian, X.L. Lu, J.M. Bai, X.G. Li, J. Mater. Chem. 14 (2004) 2787.
[32] J.J. Urban, L. Ouyang, M.H. Jo, D.S. Wang, H.K. Park, Nano Lett. 4 (2004) 1547.
[33] J.Q. Li, W.A. Sun, W.Q. Ao, J.N. Tang, J. Magn. Magn. Mater. 302 (2006) 463.
[34] A. Munoz, J.A. Alonso, M.T. Casais, M.J. Martinez-Lope, J.L. Martinez, M.T. Fernandez-Diaz, Phys. Rev. B 65 (2002) 144423-1.
[35] T. Kasuga, M. Hiramatsu, A. Hoson, T. Sekino, K. Niihara, Langmuir 14 (1998) 3160.
[36] Y. Chen, H.M. Yuan, G. Tian, G.H. Zhang, S.H. Feng, J. Solid State Chem. 180 (2007) 167.